Reduction-Induced Synthesis of Reduced Graphene Oxide-Wrapped Cu 2 O/Cu Nanoparticles for Photodegradation of Methylene Blue

Article · February 2021

DOI: 10.1021/acsanm.0c03320

8 authors, including:

Dhammike Dissanayake
University of Colombo
64 PUBLICATIONS **1,519** CITATIONS

SEE PROFILE

Charith Jayathilaka
University of Kelaniya
54 PUBLICATIONS **189** CITATIONS

SEE PROFILE

Dilushan Jayasundara
University of Colombo
32 PUBLICATIONS **222** CITATIONS

SEE PROFILE

ACS APPLIED NANO MATERIALS

www.acsanm.org Article

Reduction-Induced Synthesis of Reduced Graphene Oxide-Wrapped Cu_2O/Cu Nanoparticles for Photodegradation of Methylene Blue

K. D. R. N. Kalubowila, M. Siyath Gunewardene, J. Lakmini Kaushalya Jayasingha, Dhammike Dissanayake, Charith Jayathilaka, J. M. Dilushan Jayasundara, Yun Gao, and J. K. D. Sumedha Jayanetti*

Cite This: https://dx.doi.org/10.1021/acsanm.0c03320 Read Online

ACCESS | Metrics & More | Article Recommendations | Supporting Information

ABSTRACT: A photocatalytic composite in powder form having nanosized Cu_2O/Cu granules wrapped in multilayered reduced graphene oxide (rGO) sheets was synthesized. The fabrication process was initiated by potentiostatic electrodeposition of n-type Cu_2O thin films on Ti substrates in an acetate bath. Peeled-off Cu_2O thin films were next subjected to ultrasonic mixing with graphene oxide (GO) by maintaining a Cu_2O/GO mass ratio of 125:10. Chemical reduction using ascorbic acid converted Cu_2O partially to Cu, while converting GO completely to rGO as confirmed by Fourier transform infrared spectroscopy (FTIR), X-ray photoelectron spectroscopy (XPS), and X-ray diffraction (XRD). Transmission electron microscopy (TEM) images of the composite confirmed the presence of Cu nanoparticles of the size of tens of nanometers within the photocatalyst, Cu_2O. The fabrication process therefore implicitly favors synthesis of nanosized Cu playing the role of a co-catalyst. The Cu_2O/Cu/rGO composite showed significantly higher ability to degrade methylene blue in solution, while the effects due to photocorrosion were minimal during a month of testing when compared with Cu_2O alone. The layered rGO provides an effective medium for transporting photoelectrons to the reactant while inhibiting photocorrosion. Furthermore, the composite demonstrated its ability to split water under visible light in the presence of methanol and creates a promising platform to further develop a variety of other photocatalytic applications.

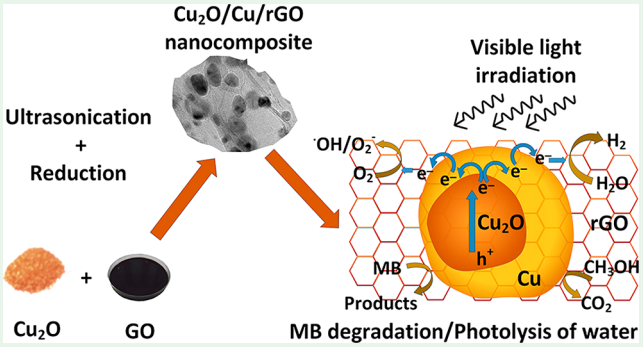

KEYWORDS: *photocatalyst, cuprous oxide, reduced graphene oxide, nanocomposite, co-catalyst*

1. INTRODUCTION

Development of photocatalytic materials in the form of harnessing solar energy has been intensely researched given its potential to drastically reduce the anthropogenic carbon footprint.[1] Sustainable use of material, scalable synthesis, biosafety, and abundance of material have become integral and important considerations in the material development process. Metal oxide semiconductors acting as photoharvesters form a broad class of photocatalytic materials, and TiO_2, ZnO, WO_3, CuO, and Cu_2O are some of the most cost-effective photocatalytic materials being researched.[2−6] Optimization of material properties enabling efficient production of electron−hole pairs from abundant solar photons, effective charge separation and transportation with minimal intermediate losses, resistance to photocorrosion, and long-term stability of the material, especially under aqueous environments, have become critically important, while careful choice of an accompanying metal co-catalyst can further enhance the associated photocatalytic redox reaction.[7,8] Fujishima and Honda in 1972 realized the first ever electrochemical photolysis of water using TiO_2,[9] and over the years the material has demonstrated its promise as an excellent photocatalyst in a variety of photocatalytic applications.[10−16] However, its wide band gap (>3.0 eV)[11,13,16] only allows harvesting the ultraviolet end of the solar spectrum,[17] making its photoelectron yield slightly low for terrestrial applications.

The placement of redox potential with respect to the semiconductor conduction and valence band (VB) energy levels has also become important in order to sustain a specific photocatalytic reaction. Therefore, band-gap re-engineering through doping, noble metal loading, or dye sensitization has become a practical requirement for enhancing the photocatalytic activity of a material.[18−21] However, such specialized treatment may seriously limit mass-scale production of the

Received: December 11, 2020
Accepted: February 12, 2021

material given the high cost of production.[22,23] Alternatively, semiconductors with a narrower band gap, for example, Cu_2O, which is one of the best metal oxides suited for terrestrial photocatalytic applications, have become attractive given the materials' earth abundance, nontoxicity, and compatibility with a variety of cost-effective scalable fabrication techniques.[2,6] Similar photocatalytic metal oxides have since been reported and used in a variety of important photoelectrochemical reactions: for example, reduction of CO_2 in the presence of water, degradation of organic pollutants in air or aqueous media, and removing heavy metals from water.[13,24,25] Synthesis of nanostructured photocatalytic materials has also attracted great attention due to the remarkable enhancement of physical and chemical properties when compared to their bulk counterpart. The increase in the surface-to-volume ratio by nanostructuring not only enables harvesting of more photons, resulting in more photoinduced electron−hole pairs, but also its nanoscale surface morphology offers shorter charge transport pathways and more redox active sites, leading to increased reaction kinetics. On the contrary, the larger surface area promotes increased defect sites at the grain boundaries, leading to increased charge recombination. Therefore, nanostructuring of materials with proper optimization remains critical to simultaneously maximize the harvested photoelectrons as well as improve the charge transport properties. To reduce undesirable electron−hole recombination or to gain high quantum efficiency, photocatalysts are often decorated with metal nanoparticle co-catalysts (Pt, Pd, Au, Rh, etc.).[8] These noble-metal nanoparticles improve charge separation and migration by forming a Schottky barrier between them and the semiconductor. It has also been reported that the metal nanoparticles such as Au and Ag exhibit strong surface plasmon resonance under visible light, significantly aiding photoharvesting of charge carriers.[20,26,27] Although somewhat susceptible to oxidation, due to earth abundance and low cost, non-noble metals such as Cu and Al have also attracted attention as co-catalysts.[28] In the present article, we report the preparation of Cu_2O thin films using electrodeposition, which enables the precise control of film morphology, crystallite size, electronic properties, and crystal facets. Furthermore, utilizing reduced graphene oxide (rGO) is explored to minimize photocorrosion. Cu_2O is naturally a p-type semiconductor due to the presence of defects such as copper vacancies or extra oxygen. However, electrodeposition brings flexibility to enable fabrication of both n-type and p-type Cu_2O films by controlling the deposition bath conditions.[29] Various methods, such as reduction of particle size and modification of surface structure, have been utilized in improving the photocatalytic activity and stability of Cu_2O-based photocatalysts.[30] However, the use of Cu_2O as a photocatalyst has been heavily limited due to its susceptibility to photocorrosion and carrier recombination.[11]

Graphene is a single layer of sp^2-hybridized carbon atoms in a hexagonal honeycomb lattice[13,15,31−33] and possesses characteristic features such as extremely high electron mobility, heat conduction, permeability to light, tensile strength, hydrophobicity, impermeability to gases and liquids, and ability to engineer surface functionalization.[34] Alternately, converting graphene oxide (GO) to reduced graphene oxide (rGO) simply removes oxygen moieties from GO, leading to properties close to those of graphene. Layering of rGO on the photocatalyst therefore has been considered as a viable option to improve stability against photocorrosion and has been tested on Cu_2O.[35] Chemical reduction of GO is one of the easier and cheaper routes for producing rGO, and is used for layering of material in large-scale production and as an alternative to pristine graphene with a variety of options for specific chemical functionalization.[34] Several studies on the synthesis of Cu_2O/rGO composites using chemical reduction have shown to enhance photocatalytic efficiency compared to pure Cu_2O; hence rGO has shown to serve as a useful electron acceptor material when combined with Cu_2O.[14,36,37] One of the earliest such work by Tran et al. reported the use of glucose for chemical reduction and the synthesized composite showed the ability to produce hydrogen.[38] Alternative chemical reduction routes have been deployed in the production of Cu_2O/rGO composites through the use of hydrazine hydrate,[39,40] wet reduction by using ascorbic acid,[13] and by using ethylene glycol.[37] Common to all of the above fabrication methodologies was the use of a solution of a copper salt and graphene oxide (GO) as starting materials. Out of the many options available for chemical reduction, only few methods are environmentally friendly.[13] Chemical reaction, photoreduction followed by solvothermal synthesis, and laser irradiation strategies are ubiquitous synthesizing methods for loading Cu nanoparticles on semiconductor photocatalysts.[28] Considering the above strategies, the method presented in this article can be mentioned as a simple way to decorate nanosized Cu_2O with Cu domains wrapped with rGO sheets without any external precursors. Once the peeled-off electrodeposited Cu_2O was added to GO, ultrasonication enabled both the homogenization as well as formation of nanosized Cu_2O particulates within the GO solution. Eventually, Cu_2O/rGO composites were synthesized through the reduction of GO to rGO and partial reduction of Cu_2O to Cu by using ascorbic acid. Consequently, the composite was tested for its photocatalytic ability to degrade methylene blue (MB) and to produce H_2 through water splitting.

2. EXPERIMENTAL SECTION

2.1. Preparation of Graphene Oxide. Graphene oxide (GO) was prepared from graphite powder (Sri Lanka Bogala vein graphite) by the improved Hummer's method.[41] In brief, a 9:1 mixture of concentrated H_2SO_4 (Sigma-Aldrich, purity 95.0−99.0%)/H_3PO_4 (Sigma-Aldrich, purity > 85.0%) and a mixture of graphite powder (18 g) and $KMnO_4$ (Sigma-Aldrich, purity > 99.0%) (6 g) were prepared. Then, the mixture of graphite powder and $KMnO_4$ was gradually added into the mixture of H_2SO_4/H_3PO_4. As this was an exothermic reaction, the temperature was maintained below 30 °C using an ice bath. Subsequently, the mixture was heated up to 50 °C and stirred for 12 h. Then, the mixture was allowed to cool to room temperature, and a mixture of ice (~400 mL) and 30% H_2O_2 (10 mL) was used to terminate the oxidation reaction. The mixture was then kept for precipitation and washed several times until its pH was around 7. Finally, a 25 mL solution of GO was poured into a Petri dish and dried to obtain a GO membrane.

2.2. Electrodeposition of Cuprous Oxide. Cu_2O was electrodeposited on Ti substrates in an acetate bath containing 0.1 M sodium acetate (Sigma-Aldrich, purity > 99.0%) and 0.01 M cupric acetate (Sigma-Aldrich, purity > 99.0%) at a potential of −200 mV with respect to the reference electrode. Initially, Ti substrates were polished with sandpaper, cleaned with a detergent, and diluted with HCl and distilled water. Then, the substrates were ultrasonically cleaned in a distilled water bath. The electrodeposition was carried out using a three-electrode system and a CS 150 CorrTest Electrochemical Workstation. A platinum plate and a saturated calomel electrode were used as the counter electrode and the reference electrode, respectively. The pH of the deposition bath was measured using a SPER Scientific pH meter and adjusted using

https://dx.doi.org/10.1021/acsanm.0c03320
ACS Appl. Nano Mater. XXXX, XXX, XXX−XXX

sodium hydroxide and acetic acid in order to obtain Cu_2O with the desired grain size and crystallite facets. Cu_2O films with micro-sized polycrystalline grains were obtained at pH 6.2.[29] The Cu_2O films prepared by this process have n-type conductivity.[42] After the deposition, samples were kept at room temperature for drying and then peeled off gently to be collected as Cu_2O powder.

2.3. Preparation of Cu_2O/rGO Composites. Different amounts of GO (1, 2.5, 5, 10, 20, and 30 mg) were added into 10 mL of distilled water and ultrasonically dissolved using a TF-650Y ultrasonic homogenizer. Next, 125 mg of Cu_2O powder was added into each GO solution and kept in the ultrasonic homogenizer for 30 min to disperse well. Then, 10 mL of ascorbic acid (0.1 M) (Sigma-Aldrich, reagent grade, crystalline) solution was added into a mixer and stirred at 60 °C for different time intervals (10, 20, 30, 40, 50, and 60 min). The fabrication process is clearly indicated in Scheme 1. Finally, the formed precipitate was washed several times with water and ethanol. The product was then dried at 60 °C.

Scheme 1. Illustration of the Formation Process of the Cu_2O/Cu/rGO Nanocomposite

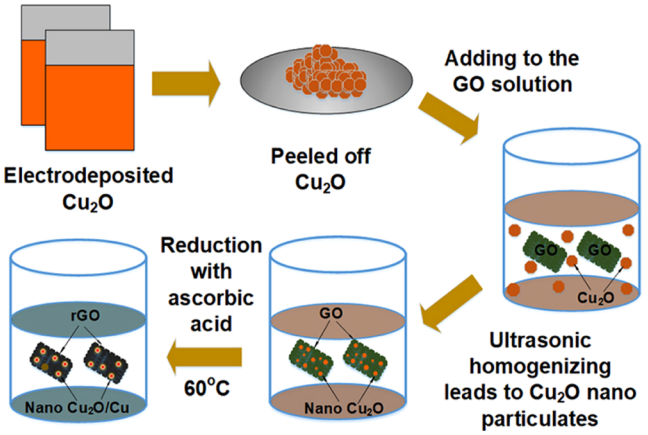

2.4. Characterization of Cu_2O/rGO Composites. The surface morphology of the composite was investigated by scanning electron microscopy (SEM) (Zeiss Evols15). Inner structures of the composite were characterized by a transmission electron microscope (TEM, H-800). The samples for TEM were prepared by dispersing the product in ethanol using a sonicator bath for 15 min and dropped on a copper grid for observation. The crystal structure was confirmed by X-ray powder diffraction (XRD) (Rigaku Ultima IV). X-ray photoelectron spectroscopy (XPS) measurements were performed using an ESCALAB 250Xi spectrometer. All of the binding energies were calibrated to the reference of the C 1s peak at 284.6 eV. Fourier transform infrared (FTIR) spectra of the samples were obtained using a Thermo Scientific Nicolet iS10 spectrometer.

2.5. Photocatalysis Measurements. *2.5.1.. Photodegradation of Methylene Blue (MB).* The photocatalytic activity of Cu_2O/rGO composites was investigated using the photodegradation of MB in water. The catalyst (20 mg) was mixed into 50 mL of MB (10 mg/L) solution and stirred well for 30 min in the dark. Then, the solution was irradiated using a 300 W xenon lamp (the photon flux at the reactor was 3.66 mW/cm^2). The reaction mixture was stirred continuously using a magnetic stirrer. At given intervals, 1 mL portions of the reaction mixture were drawn out for analysis. These samples were centrifuged to remove the dispersed catalyst powder and analyzed for MB by using ultraviolet−visible (UV−vis) spectroscopy (Ocean Optics, FLAME-T-UV−VIS−ES).

2.5.2.. Photocatalytic H_2 Production. The Cu_2O/Cu/rGO composites were produced at selected reduction durations (20, 30, and 40 min) and evaluated for their ability to produce H_2. A mixture of 20 mL of methanol and 80 mL of water was used in the reactor with 20 mg of the composite. The reactor was maintained at 25 °C during the evolution of H_2. The gas products were analyzed and quantified using GC Smart (GC-2018) Shimadzu gas chromatography (GC). After every 60 min, 200 μL of gas was taken from the samples using a gas-tight syringe and was injected into a gas chromatograph to identify the gaseous products during the photocatalytic reaction using a thermal conductivity detector with argon as the carrier gas. The sample was irradiated by a xe lamp (300 W). The light intensity was measured with a thermophile sensor (818P-001-12, Newport) and fixed at 100 mW/cm^2 by controlling the distance between the reactor and the lamp.

3. RESULTS AND DISCUSSION

Electrodeposition allows control of both the conductivity type and the surface morphology of the deposited films by controlling the pH of the deposition bath. A detailed study on the change of conductivity type of the electrodeposited Cu_2O with bath pH has been conducted.[29] Figure 1a shows an SEM image of an electrodeposited Cu_2O thin film deposited at pH 6.2. When electrodeposited at pH 6.2, Cu_2O has n-type conductivity and the alignment of bands referenced to vacuum are reported to be at −4.19 and −6.29 eV for the conduction band (CB) and the valence band, respectively.[29] The morphological features of the deposited thin films show microsized grains dominated by truncated octahedral shapes. It can be seen that the surface morphology of the peeled-off films has changed due to the release of strain, as shown in Figure 1b. However, it can also be seen that, on average, the grain sizes remain the same. The synthesized Cu_2O/rGO composite in

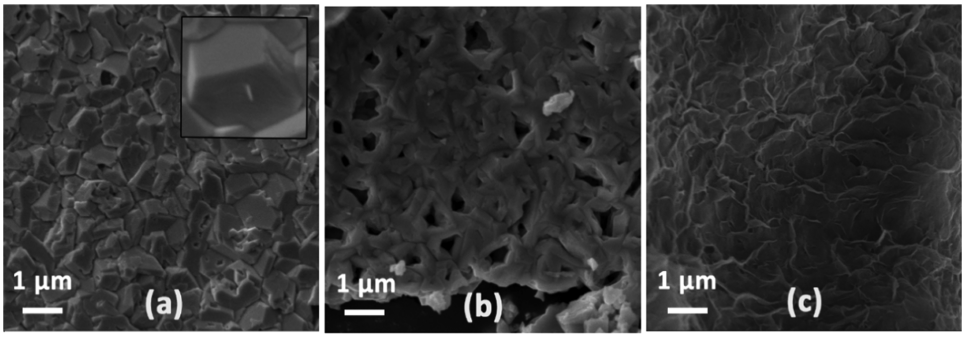

Figure 1. SEM images of Cu_2O thin films (a) electrodeposited on a Ti substrate in an acetate bath containing 0.1 M sodium acetate and 0.01 M cupric acetate at pH 6.2 for 40 min (the inset shows the zoomed image of the Cu_2O grain); (b) the same film after being peeled off from the substrate; and (c) Cu_2O/rGO composite in a powder form synthesized by ultrasonically homogenizing the peeled-off electrodeposited Cu_2O thin films and GO and subsequently reducing using 0.1 M ascorbic acid.

https://dx.doi.org/10.1021/acsanm.0c03320
ACS Appl. Nano Mater. XXXX, XXX, XXX−XXX

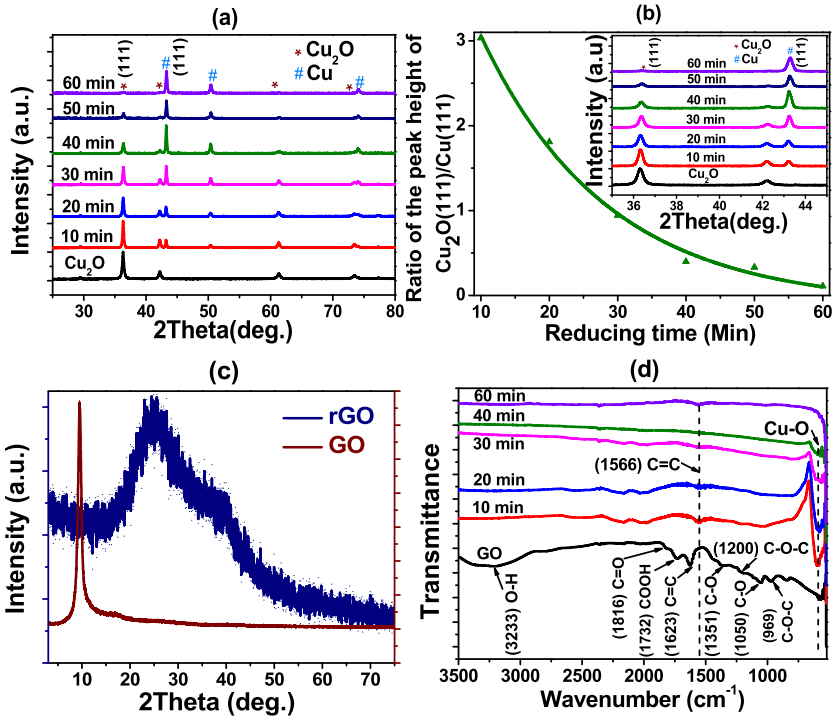

Figure 2. (a) XRD patterns comparing electrodeposited pure n-type Cu_2O with Cu_2O/Cu/rGO composites synthesized by ultrasonically homogenizing peeled-off electrodeposited Cu_2O thin films and GO, subsequently being reduced using 0.1 M ascorbic acid for 10, 20, 30, 40, 50, and 60 min, respectively, and maintaining an initial GO/Cu_2O mass ratio of 10:125. (b) Variation of the XRD peak height ratio of Cu_2O(111) to Cu(111) in Cu_2O/Cu/rGO composites with reduction time (the inset shows an enlarged image of the XRD spectral peaks related to the (111) phase of Cu_2O and Cu). (c) XRD patterns of as-synthesized GO using the improved Hummers' method and chemically synthesized rGO reduced by ascorbic acid for 30 min. (d) FTIR spectra of the synthesized GO and Cu_2O/Cu/rGO composites produced at different reducing durations (10, 20, 30, 40, 50, 60 min) with ascorbic acid.

Figure 1c shows a more uniform surface morphology due to the formation of the rGO layer.

The structural properties of the composite evaluated by XRD measurements (see Figure 2a) showed the presence of Cu_2O from the observed characteristic peaks at 29.4° (110), 36.3° (111), 42.18° (200), 61.26° (220), and 73.48° (311), where the (111) peak was the most intense XRD peak. Furthermore, the composite prepared by reducing the Cu_2O and GO mixture retained the crystalline phase of Cu_2O, while showing the emergence of a Cu(111) peak. It can be observed that, with increasing reduction time, the intensity of the (111) XRD peak of Cu_2O decreases and that of the Cu(111) peak increases, confirming the reduction of Cu_2O to Cu with ascorbic acid. This indicates that the reaction time with ascorbic acid controls the ratio of Cu_2O/Cu phases in the composite. In order to capture the dynamics of the reduction process, the XRD spectral peak intensity ratio of Cu_2O(111)/Cu(111) vs reaction time is plotted (see Figure 2b). An exponential decay of the ratio Cu_2O(111):Cu(111) can be observed, while the Cu_2O(111) peak almost entirely disappears after reacting with ascorbic acid for 60 min. It was confirmed in a separate experiment using XRD that GO reduces to rGO when reacted with ascorbic acid in a duration less than 30 min. It could be observed that GO having a single XRD peak at 9.5° disappeared with the growth of a broader XRD hump around 24.5° due to the formation of rGO. The broadened peak further indicated that graphene had exfoliated into a few-layered sheet-like structure of rGO (see Figure 2c).

To further analyze the active functional groups of synthesized rGO, FTIR spectra were collected for Cu_2O/Cu/rGO composites synthesized under varied reduction levels (see Figure 2d). It can be observed that the oxygen functionalities in the composite are initially apparent but subside with increased reduction. The FTIR spectrum of the synthesized GO showed a strong band around 3233 cm^{-1}, primarily associated with the stretching vibrations of the O−H group. Other features were assigned to the C═O carboxylic acid stretching at 1732 cm^{-1}, the C−OH stretching at 1351 cm^{-1}, the sp^2 structure of the unoxidized graphitic domains at 1623 cm^{-1}, the C−O stretching of Ar−OH groups at 1200 cm^{-1}, and the C−O stretching at 1050 cm^{-1}. Reduction of the composite leads to a decrease in the absorption bands of the O−H group, C═O group, C−O group, and C−OH group. The C═C peak for GO typically occurs around 1623 cm^{-1}. However, the reduction of GO shifts the C═C related peak of rGO to 1566 cm^{-1}, which confirms the restoration of the sp^2 carbon network, and the observations were consistent with that reported in the literature.[43] The absorption band at 582 cm^{-1} in the Cu_2O/rGO composite can be ascribed to the stretching vibration of Cu−O. This indicates the existence of Cu_2O at intermediate stages of the reduction process. When the reducing time reaches 60 min, the absorption peak of Cu−O disappears entirely, indicating the complete reduction of Cu_2O to Cu.

X-ray photoelectron spectroscopy (XPS) measurements were carried out to investigate the composition and chemical states of the Cu_2O/Cu/rGO composite reduced using ascorbic acid for 30 min. The corresponding XPS spectra for Cu and C are shown in Figure 3. The spectral peaks positioned at 932.4 and 934.4 eV correspond to the Cu $2p_{3/2}$, indicating the

https://dx.doi.org/10.1021/acsanm.0c03320
ACS Appl. Nano Mater. XXXX, XXX, XXX−XXX

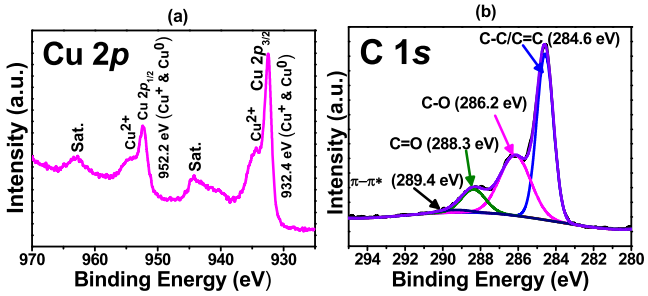

Figure 3. XPS spectra of (a) Cu 2p and (b) C 1s of the Cu_2O/Cu/rGO composites synthesized by ultrasonically homogenizing peeled-off electrodeposited Cu_2O films and GO, subsequently being reduced using 0.1 M ascorbic acid for 30 min.

presence of Cu^+/Cu^0 with a peak intensity of 38.7% and Cu^{2+} states with a peak intensity of 48.5%, respectively, in the composite (the binding energy resolution was insufficient to deconvolute the $2p_{3/2}$ peaks of Cu^+ and Cu^0). The 952.2 eV (Cu^+/Cu^0) and 954.4 eV (Cu^{2+}) peaks (see Figure 3a) correspond to the Cu $2p_{1/2}$. Also, two satellite peaks appearing at 943.9 and 962.9 eV positions support the presence of the Cu^{2+} state. The presence of the Cu^{2+} state only in the XPS measurements indicates that the Cu^{2+} state is limited only to the surface of the formed composite particles. The absence of CuO or $Cu(OH)_2$ peaks in the XRD patterns clearly indicates that the bulk composite has not been influenced by the Cu^{2+} state. The obtained C 1s spectra were deconvoluted into four distinct peaks positioned at 284.6, 286.2, 288.3, and 289.4 eV having relative peak intensities of 52.7, 34, 10, and 3.2%, respectively. It was evident that the peak intensities at 289.4 eV (indicative of C═O) and 286.2 eV (indicative of C−O) were both significantly lower compared to that of the peak at 284.6 eV (indicative of both C═C and C−C). A similar comparison was made using the C 1s spectra reported for GO[44] synthesized using Bogala vein graphite, the same precursor and the process used in our experiment. Clearly, the C═O and C−O associated peaks for GO were significantly more pronounced compared to the peak associated with C═O and C−O. This observation provided further evidence of reduction of GO in the synthesized composite and is consistent with the observations made on related work that used ascorbic acid as a reductant.[45]

The photocatalytic activity of the composite was tested by quantification of MB degradation. A xenon lamp was used to generate a broad-wavelength excitation source. A 10 mg/L MB solution was illuminated with the xenon source continuously for 2 h. After each predefined duration, small quantities of MB were extracted from the reactor and centrifuged to remove any residual photocatalyst. Thereafter, the absorption spectra were measured using a UV−vis spectrophotometer to evaluate the photodegradation of MB. The peaks of the collected absorption spectra were consistently located around 668 nm, which can be associated with the π-system of MB. However, to quantify the degradation of MB, the area subtended by the respective absorbance spectra in the range from 550 to 750 nm was measured in order to acquire a cumulative absorbance measure. Each of such estimates was then normalized with respect to the cumulative absorbance measured for the initial MB solution without illumination. The yielded normalized cumulative absorbance, A_{abs}, was thereafter converted to a percentage degradation fraction $100(1 - A_{abs})$. This

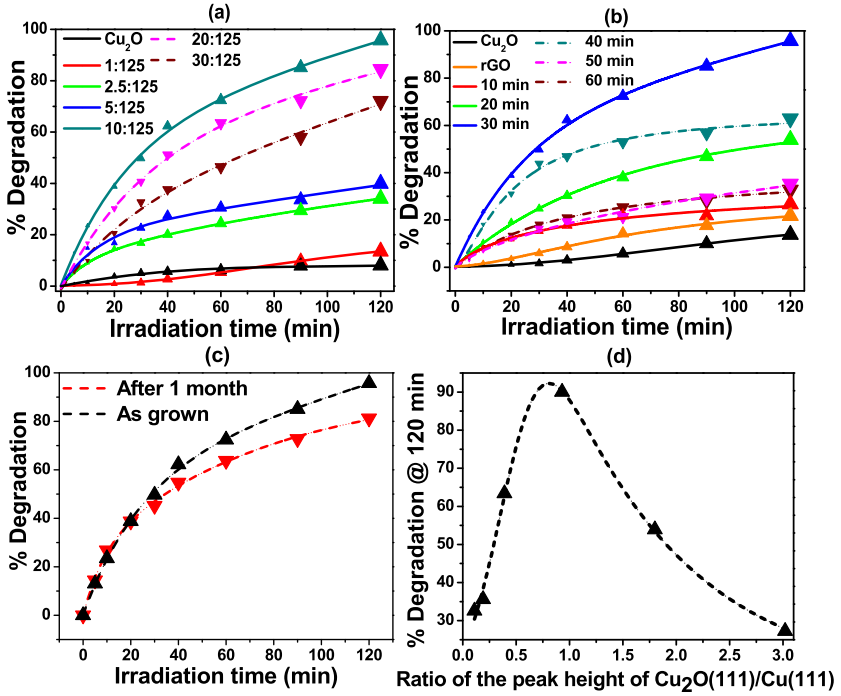

Figure 4. Percentage degradation of MB under the irradiation of visible light using a 300 W xenon lamp with Cu_2O/rGO composites (a) synthesized with different mass ratios of GO to Cu_2O (1, 2.5, 5, 10, 20, 30:125) and reduced using ascorbic acid (0.1 M) for 30 min, and (b) reduced with varied durations (10, 20, 30, 40, 50, 60 min) with 0.1 M ascorbic acid having an initial GO to Cu_2O mass ratio of 10:125. (c) Percentage degradation of MB under the irradiation of visible light with as-synthesized Cu_2O/Cu/rGO and composite kept for 1 month. (d) Variation of the percentage degradation of MB at the irradiation time of 120 min with the ratio of the corresponding peak heights of $Cu_2O(111)$ to Cu(111) extracted from the XRD patterns in Figure 2b. Solid lines show the best fits to the corresponding data points.

https://dx.doi.org/10.1021/acsanm.0c03320
ACS Appl. Nano Mater. XXXX, XXX, XXX−XXX

percentage degradation fraction was measured at predefined time stamps of 5, 10, 20, 30, 40, 60, 90, 120 min during illumination for each of the Cu_2O/rGO composites having different initial mass ratios of GO to Cu_2O (1, 2.5, 5, 10, 20, 30:125). Figure 4a confirms that increasing GO eventually leads to a decrease in the degradation efficiency, which can be attributed to the enhanced absorption and scattering of photons by the excess carbon present in the composite.[46] The highest degradation percentage was reported for the composite synthesized with a GO to Cu_2O ratio of 10:125 (see Figure 4a); hence, for subsequent synthesis of the composite and measurements the same ratio was maintained.

In order to further optimize the photocatalytic activity of the composite, MB degradation percentages were measured for the composites prepared using different reduction times (10, 20, 30, 40, 50, and 60 min). The photocatalytic activities of these composites were compared with the photocatalytic activities of Cu_2O and rGO separately. The composites showed significantly higher degradation ability of MB as compared to Cu_2O and rGO taken alone (see Figure 4b). The absorption spectra of MB degraded for different times using the composite (composite having the initial mass ratio of GO/Cu_2O 10:125 and reduced for 30 min) are shown in the Supporting Information Figure S1. The inset of the figure shows the digital photographs of the MB solutions at different irradiation time intervals. Figure 4c compares the percentage degradation of MB (at different photocatalytic reaction times) of a freshly prepared composite with the same sample re-used after 1 month. Before being reused and tested, the sedimented composite was dried and stored for a duration of 1 month under ambient conditions. The percentage of degradation after one month was well within 20% of the initial value, indicating that the composite is relatively stable. It can be inferred that the layering of rGO would have significantly contributed towards the stability of the material. The claim can be further supported by some of the previous studies that investigated the decreased oxidation of Cu_2O under aqueous conditions after layering with rGO.[38] A reduction time of 30 min was found to produce the most active composite catalyst for the degradation of MB and this composite had a ratio of Cu_2O/Cu ≈ 1:1 as observed in the XRD patterns (Figure 4d).

To further probe the internal morphology of the material, TEM imaging was performed on Cu_2O/Cu/rGO composites (synthesized with 30 min reduction using 0.1 M ascorbic acid and having an initial mass ratio of GO/Cu_2O=10:125) (see Figure 5). TEM images confirmed that the size distribution of the particles on average was around ∼10 to 20 nm, while thin sheets of rGO wrapped around the nanosized Cu_2O/Cu particles. The formation of ultrasmall particulates (with dimensions as small as 10 nm) was due to the rigorous sonication process introduced during the mixing of GO and Cu_2O prior to reduction. Starting from Cu_2O nanocolloids, synthesis of Cu nanoparticles using ascorbic acid-aided reduction has been previously reported.[47] The Cu_2O (in powder form) precursor used in our study was of much larger size (more than the microscale); therefore, it can be inferred that the ultrasonication is the predominant factor aiding the formation of nanosized Cu domains in the composite as observed by TEM. The TEM images in Figure 5a clearly show two distinct contrasting areas in the nanoparticles. These contrasting areas in TEM images can therefore be used to distinguish between Cu and Cu_2O.[48] The electron-dense Cu should lead to brighter regions, while the darker regions would

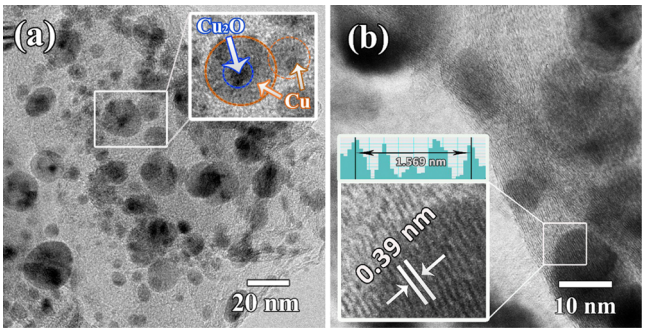

Figure 5. (a) TEM images of the Cu_2O/Cu/rGO composite synthesized by ultrasonically homogenizing GO and peeled-off electrodeposited Cu_2O thin films (deposited on Ti substrates in an acetate bath of pH 6.2) having an initial mass ratio of GO/Cu_2O=10:125 and subsequently reduced using 0.1 M ascorbic acid for 30 min; the inset shows a typical Cu_2O/Cu nanoparticle; (b) an area of the composite showing many-layered rGO; the inset shows the interlayer separation of rGO sheets. Here, the average interlayer spacing was measured to be 0.39 ± 0.06 nm.

correspond to Cu_2O. Most of the grains shown in the TEM images are indicative of the presence of nanosized Cu regions along with Cu_2O after the reduction process. Furthermore, several nanoparticles show only brighter areas indicative of some Cu_2O nanoparticles being completely converted into Cu during the reduction process. Previous studies show that these nanosized Cu domains could facilitate optical phenomena such as localized surface plasmon resonance (LSPR). Therefore, the effect could significantly assist photogenerated electrons to efficiently participate in the related redox reaction. Literature studies also show that Cu nanoparticles can produce LSPR in a long range of visible wavelengths, which can be tuned by controlling the particle size. From an electronic band perspective, the metal nanoparticles assist in excitation of electron−hole pairs between the d-band of the metal and the conduction band of the semiconductor (interband excitation).[49−51] Cu_2O/Cu nanoparticles densely scattered on the wrinkled graphene sheets are clearly observed in Figure 5a. A typical cross-sectional profile of a multilayered rGO sheet can be seen in Figure 5b, while further analysis yielded an intersheet separation of 0.39 ± 0.06 nm consistent with the literature.[52] The composite also remained stable under aqueous conditions, and even after 1 month the material retained 80% of its ability to degrade MB, implying that the photocorrosion is minimal (see Figure 4c).

To summarize, an energy-level diagram showing the position of the bands of the electrodeposited Cu_2O is presented in Figure 6 with respect to the vacuum level found in our previous investigations.[29] Furthermore, related reactions for MB degradation and H_2 generation by water splitting in the presence of methanol are depicted. When exposed to light, Cu_2O generates electron and hole pairs in the conduction band (CB) and valence band (VB). Reduction-induced Cu sites on the Cu_2O nanoparticles act as co-catalysts and improve the charge separation mechanism. These Cu nanoparticles also open a pathway to transfer the photogenerated electrons into rGO sheets with minimal losses. Also, the rGO sheets act as an electron acceptor and transporter, providing a path for the electrons to generate reactive oxidation species such as $^{\bullet}OH$ and O_2^-. Therefore, Cu nanoparticles facilitate minimization of the charge carrier recombination and help produce more reactive species. These reactive species promote the MB

https://dx.doi.org/10.1021/acsanm.0c03320
ACS Appl. Nano Mater. XXXX, XXX, XXX−XXX

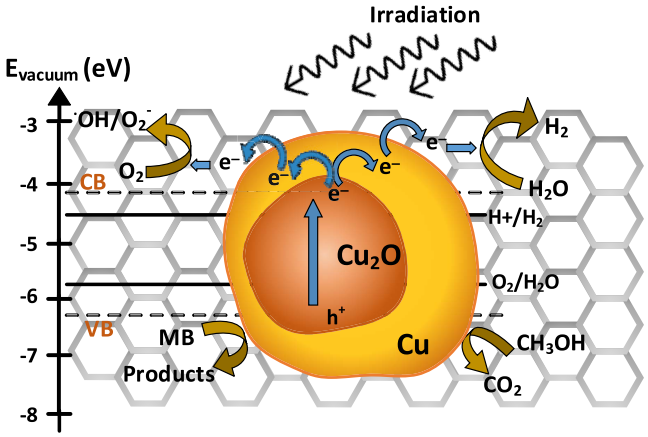

Figure 6. Energy-level diagram and the electron transport in the degradation of MB and the photolysis of water in sacrificial mode with methanol, using Cu_2O/Cu/rGO composite as a photocatalyst.

degradation into intermediate products. In order to evaluate the co-catalytic contribution of the nanosized Cu domains, a control experiment was performed. The percentage degradation of MB after 2 h of irradiation for nanosized Cu_2O/Cu/rGO was as much as 70% higher compared to the composite without Cu (see Supporting Information Figure S2). Therefore, the critical role played by the metal co-catalyst was further highlighted by this fact.

When considering the H_2 evolution reaction, the sacrificial donor, methanol, consumes holes in the VB by leaving an electron in the CB of Cu_2O. Partial reduction of Cu_2O creates Cu islands on Cu_2O particles, facilitating the separation of carriers and thus enhancing the photocatalytic activity. Graphene, having a high electron mobility due to its two-dimensional π-conjugated structure, acts as an electron collector and a transporter. It also separates the electrons and transfers them to reaction sites and improves H_2 production. Graphene layers wrapped around the composite significantly limit self-reduction/oxidation and preserve Cu_2O, which is prone to photocorrosion. The composite was subsequently evaluated for its ability to split water into H_2 and O_2. The H_2 evolution reaction had to be facilitated using methanol as a hole scavenger. To measure the ability to evolve H_2, 20 mg of each composite reduced for 20, 30, and 40 min, respectively, was separately mixed in 100 mL of water/methanol mixture (volume ratio = 4:1). The evolved H_2 was measured every hour using a a gas chromatograph for a duration of 7 h (see Supporting Information Figure S3). The composite, reduced for 30 min, evolved 0.9 μmol of H_2 during 7 h, which was the highest. No significant changes were observed in the measured XRD spectra of the composite before and after 8 h of H_2 evolution (see Supporting Information Figure S4), indicating that the structural properties of the composite remained stable during photocatalysis. The H_2 evolution measurements were done under isothermal conditions in which the bath temperature was maintained around 25 °C. Therefore, it should be noted here that the possibility of a methanol-reforming reaction, which occurs at much higher temperatures,[53] can be safely ruled out. Dye sensitization also plays an important role in the enhancement of photocatalysis.[54] During the MB degradation, this effect may further enhance the photocatalytic degradation. However, the composite's ability to evolve H_2 by splitting water proves that any possible photocatalytic enhancement due to dye sensitization is only supplementary and hence not a significant factor that determines the overall photocatalytic behavior.

4. CONCLUSIONS

A nanosized Cu_2O/Cu/rGO photocatalytic composite, sensitive to visible light, was synthesized using an electrodeposition-assisted chemical reduction route. Compared to pure, n-type Cu_2O thin films, the composite showed significantly high degradation ability of methylene blue in an aqueous medium. The composite was also stable under the tested conditions. As synthesis precursors, n-type Cu_2O thin films were initially electrodeposited on a Ti substrate and were peeled off before mixing with GO and distilled water. Ultrasonic homogenization converted the peeled-off n-type Cu_2O to nanosized particles dispersed in the GO solution. Consequently, the mixture was chemically reduced using ascorbic acid to produce the desired Cu_2O/Cu/rGO photocatalytic composite. TEM images confirmed the presence of nanosized Cu_2O/Cu wrapped in multilayered rGO. Chemical reduction helped simultaneously to convert GO to rGO, while Cu_2O was partially converted to Cu. Best photocatalytic activity was reported for the composites prepared with an initial Cu_2O/GO mixture having a mass ratio of 125:10 and reduced using 0.1 M ascorbic acid for 30 min. The photocatalytic enhancement due to Cu in the composite was confirmed by comparing the percentage of MB degradation with that of the pure photocatalyst Cu_2O loaded on rGO. This enhancement can be attributed to the nanosized Cu acting as a co-catalyst and providing centers for efficient charge transfer. Furthermore, rGO in the composite acts as an electron acceptor with a smaller charge transfer resistance improving the interfacial electron transfer process. Therefore, both rGO and Cu contribute to the overall improvement of the photocatalytic activity of the composite. It is also worth noting that in this study, ascorbic acid, which is typically used for reducing GO, had been used simultaneously to reduce Cu_2O to Cu. This, as we perceive, is a novel route to load a co-catalyst in a photocatalyst with the least intervention, while making the fabrication process simpler. Though not comprehensively tested, it was experimentally confirmed that the composite produced H_2 by splitting water under solar irradiation when the redox reaction was assisted by a sacrificial agent such as methanol. The composite therefore becomes an ideal platform to test many photocatalytic applications that heavily rely upon visible light.

■ ASSOCIATED CONTENT

Supporting Information

The Supporting Information is available free of charge at https://pubs.acs.org/doi/10.1021/acsanm.0c03320.

Absorption spectra of the Cu_2O/Cu/rGO nanocomposite showing the time dependence of the amount of degradation in MB and the digital photographs of consequent discoloration of MB; comparison tests for the degradation of MB in the presence of the Cu_2O/Cu/rGO nanocomposite, Cu_2O, rGO, and Cu_2O/rGO; H_2 evolution measurements of the Cu_2O/Cu/rGO nanocomposites synthesized at different reduction durations (20, 30, 40 min); and XRD patterns of Cu_2O/Cu/rGO nanocomposite before and after the H_2 evolution process (PDF)

https://dx.doi.org/10.1021/acsanm.0c03320
ACS Appl. Nano Mater. XXXX, XXX, XXX−XXX

AUTHOR INFORMATION

Corresponding Author

J. K. D. Sumedha Jayanetti − *Department of Physics and Department of Instrumentation & Automation Technology, University of Colombo, Colombo 00300, Sri Lanka;* orcid.org/0000-0003-4961-0902; Phone: +94714406281; Email: sumedhajayanetti@gmail.com

Authors

K. D. R. N. Kalubowila − *Department of Physics, University of Colombo, Colombo 00300, Sri Lanka;* orcid.org/0000-0003-3444-223X

M. Siyath Gunewardene − *Department of Physics, University of Colombo, Colombo 00300, Sri Lanka*

J. Lakmini Kaushalya Jayasingha − *Department of Instrumentation & Automation Technology, University of Colombo, Colombo 00300, Sri Lanka; Ministry of Education Key Laboratory for the Green Preparation and Application of Fundamental Materials, School of Materials Science & Engineering, Hubei University, Wuhan 430062, China*

Dhammike Dissanayake − *Department of Chemistry, University of Colombo, Colombo 00300, Sri Lanka;* orcid.org/0000-0002-6213-5782

Charith Jayathilaka − *Department of Physics, University of Kelaniya, Kelaniya 11600, Sri Lanka*

J. M. Dilushan Jayasundara − *Department of Physics, University of Colombo, Colombo 00300, Sri Lanka;* orcid.org/0000-0001-9220-1130

Yun Gao − *Ministry of Education Key Laboratory for the Green Preparation and Application of Fundamental Materials, School of Materials Science & Engineering, Hubei University, Wuhan 430062, China;* orcid.org/0000-0002-9898-5690

Complete contact information is available at: https://pubs.acs.org/10.1021/acsanm.0c03320

Notes

The authors declare no competing financial interest.

ACKNOWLEDGMENTS

Financial assistance from the research grant of the National Research Council (NRC/16-094) is gratefully acknowledged. The kind assistance given for XRD measurements by Prof. Nilwala Kottegoda of the Department of Chemistry and the Center for Advance Materials Research, Faculty of Applied Science at the University of Sri Jayewardenepura, Sri Lanka, is also specially acknowledged. Furthermore, TEM-related services rendered by the Sri Lanka Institute of Nanotechnology (SLINTEC) are acknowledged.

REFERENCES

(1) Gray, H. B. Powering the planet with solar fuel. *Nat. Chem.* **2009**, *1*, No. 7.

(2) Siripala, W.; Ivanovskaya, A.; Jaramillo, T. F.; Baeck, S. H.; McFarland, E. W. A Cu_2O/TiO_2 heterojunction thin film cathode for photoelectrocatalysis. *Sol. Energy Mater. Sol. Cells* **2003**, *77*, 229−237.

(3) Wolcott, A.; Smith, W. A.; Kuykendall, T. R.; Zhao, Y.; Zhang, J. Z. Photoelectrochemical Study of Nanostructured ZnO Thin Films for Hydrogen Generation from Water Splitting. *Adv. Funct. Mater.* **2009**, *19*, 1849−1856.

(4) Maruthamuthu, P.; Ashokkumar, M. Hydrogen generation using Cu (II)/WO3 and oxalic acid by visible light. *Int. J. Hydrogen Energy* **1988**, *13*, 677−680.

(5) Li, B.; Wang, Y. Facile synthesis and photocatalytic activity of ZnO−CuO nanocomposite. *Superlattices Microstruct.* **2010**, *47*, 615−623.

(6) Bagal, I. V.; Chodankar, N. R.; Hassan, M. A.; Waseem, A.; Johar, M. A.; Kim, D.-H.; Ryu, S.-W. Cu_2O as an emerging photocathode for solar water splitting - A status review. *Int. J. Hydrogen Energy* **2019**, *44*, 21351−21378.

(7) Al-Azri, Z. H.; Chen, W. T.; Chan, A.; Jovic, V.; Ina, T.; Idriss, H.; Waterhouse, G. I. The roles of metal co-catalysts and reaction media in photocatalytic hydrogen production: Performance evaluation of M/TiO_2 photocatalysts (M = Pd, Pt, Au) in different alcohol−water mixtures. *J. Catal.* **2015**, *329*, 355−367.

(8) Wang, Y.; Chen, Y.; Hou, Q.; Ju, M.; Li, W. Coupling Plasmonic and Cocatalyst Nanoparticles on $N-TiO_2$ for Visible-Light-Driven Catalytic Organic Synthesis. *Nanomaterials* **2019**, *9*, No. 391.

(9) Fujishima, A.; Honda, K. Photolysis-decomposition of water at the surface of an irradiated semiconductor. *Nature* **1972**, *238*, 37−38.

(10) Hashimoto, K.; Irie, H.; Fujishima, A. TiO_2 Photocatalysis: A Historical Overview and Future Prospects. *Jpn. J. Appl. Phys.* **2005**, *44*, 8269−8285.

(11) Xu, L.; Xu, H.; Wu, S.; Zhang, X. Synergy effect over electrodeposited submicron Cu_2O films in photocatalytic degradation of methylene blue. *Appl. Surf. Sci.* **2012**, *258*, 4934−4938.

(12) Darvishi, M.; Seyed-Yazdi, J. Characterization and comparison of photocatalytic activities of prepared TiO_2/graphene nanocomposites using titanium butoxide and TiO2 via microwave irradiation method. *Mater. Res. Express* **2016**, *3*, No. 085601.

(13) Li, B.; Liu, T.; Hu, L.; Wang, Y. A facile one-pot synthesis of Cu_2O/RGO nanocomposite for removal of organic pollutant. *J. Phys. Chem. Solids* **2013**, *74*, 635−640.

(14) Gao, Z.; Liu, J.; Xu, F.; Wu, D.; Wu, Z.; Jiang, K. One-pot synthesis of graphene−cuprous oxide composite with enhanced photocatalytic activity. *Solid State Sci.* **2012**, *14*, 276−280.

(15) Yadav, H. M.; Kim, J. S. Solvothermal synthesis of anatase TiO_2-graphene oxide nanocomposites and their photocatalytic performance. *J. Alloys Compd.* **2016**, *688*, 123−129.

(16) Alim, N. S.; Lintang, H. O.; Yuliati, L. Photocatalytic removal of phenol over titanium dioxide- reduced graphene oxide photocatalyst. *IOP Conf. Ser.: Mater. Sci. Eng.* **2016**, *107*, No. 012001.

(17) Zhang, W.; Li, X.; Yang, Z.; Tang, X.; Ma, Y.; Li, M.; Hu, N.; Wei, H.; Zhang, Y. In situ preparation of cubic Cu_2O-RGO nanocomposites for enhanced visible-light degradation of methyl orange. *Nanotechnology* **2016**, *27*, No. 265703.

(18) Zhang, F.; Wang, X.; Liu, H.; Liu, C.; Wan, Y.; Long, Y.; Cai, Z. Recent Advances and Applications of Semiconductor Photocatalytic Technology. *Appl. Sci.* **2019**, *9*, No. 2489.

(19) Piyadasa, A.; Wang, S.; Gao, P.-X. Band structure engineering strategies of metal oxide semiconductor nanowires and related nanostructures: A review. *Semicond. Sci. Technol.* **2017**, *32*, No. 073001.

(20) Wang, P.; Huang, B.; Dai, Y.; Whangbo, M.-H. Plasmonic photocatalysts: harvesting visible light with noble metal nanoparticles. *Phys. Chem. Chem. Phys.* **2012**, *14*, No. 9813.

(21) Zhang, W.; Li, Y.; Zeng, X.; Peng, S. Synergetic effect of metal nickel and graphene as a cocatalyst for enhanced photocatalytic hydrogen evolution via dye sensitization. *Sci. Rep.* **2015**, *5*, No. 10589.

(22) Ahmad, R.; Ahmad, Z.; Khan, A. U.; Mastoi, N. R.; Aslam, M.; Kim, J. Photocatalytic systems as an advanced environmental remediation: Recent developments, limitations and new avenues for applications. *J. Environ. Chem. Eng.* **2016**, *4*, 4143−4164.

(23) Goto, Y.; Hisatomi, T.; Wang, Q.; Higashi, T.; Ishikiriyama, K.; Maeda, T.; Sakata, Y.; Okunaka, S.; Tokudome, H.; Katayama, M.; Akiyama, S.; Nishiyama, H.; Inoue, Y.; Takewaki, T.; Setoyama, T.; Minegishi, T.; Takata, T.; Yamada, T.; Domen, K. A Particulate Photocatalyst Water-Splitting Panel for Large-Scale Solar Hydrogen Generation. *Joule* **2018**, *2*, 509−520.

(24) An, X.; Li, K.; Tang, J. Cu_2O/Reduced Graphene Oxide Composites for the Photocatalytic Conversion of CO_2. *ChemSusChem* **2014**, *7*, 1086−1093.
(25) Eisenberg, R.; Gray, H. B.; Crabtree, G. W. Addressing the challenge of carbon-free energy. *Proc. Natl. Acad. Sci. U.S.A.* **2020**, *117*, 12543−12549.
(26) Hou, W.; Cronin, S. B. A Review of Surface Plasmon Resonance-Enhanced Photocatalysis. *Adv. Funct. Mater.* **2013**, *23*, 1612−1619.
(27) Clavero, C. Plasmon-induced hot-electron generation at nanoparticle/metal-oxide interfaces for photovoltaic and photocatalytic devices. *Nat. Photonics* **2014**, *8*, 95−103.
(28) Jiang, Q.; Ji, C.; Riley, D. J.; Xie, F. Boosting the Efficiency of Photoelectrolysis by the Addition of Non-Noble Plasmonic Metals: Al & Cu. *Nanomaterials* **2019**, *9*, No. 1.
(29) Kalubowila, K. D. R. N.; Jayathileka, K. M. D. C.; Kumara, L. S. R.; Ohara, K.; Kohara, S.; Sakata, O.; Gunewardene, M. S.; Jayasundara, J. M. D. R.; Dissanayake, D. P.; Jayanetti, J. K. D. S. Effect of Bath pH on Electronic and Morphological Properties of Electrodeposited Cu_2O Thin Films. *J. Electrochem. Soc.* **2019**, *166*, D113−D119.
(30) Seema, H.; Kemp, K. C.; Chandra, V.; Kim, K. S. Graphene−SnO_2 composites for highly efficient photocatalytic degradation of methylene blue under sunlight. *Nanotechnology* **2012**, *23*, No. 355705.
(31) Xiang, Q.; Yu, J.; Jaroniec, M. Graphene-based semiconductor photocatalysts. *Chem. Soc. Rev.* **2012**, *41*, 782−796.
(32) Ji, Z.; Shen, X.; Li, M.; Zhou, H.; Zhu, G.; Chen, K. Synthesis of reduced graphene oxide/CeO_2 nanocomposites and their photocatalytic properties. *Nanotechnology* **2013**, *24*, No. 115603.
(33) Zhu, Y.; Murali, S.; Cai, W.; Li, X.; Suk, J. W.; Potts, J. R.; Ruoff, R. S. Graphene and Graphene Oxide: Synthesis, Properties, and Applications. *Adv. Mater.* **2010**, *22*, 3906−3924.
(34) Boukhvalov, D. W.; Katsnelson, M. I. Chemical functionalization of graphene. *J. Phys.: Condens. Matter* **2009**, *21*, No. 344205.
(35) Bai, W.; Wu, M.; Du, X.; Gong, W.; Ding, Y.; Song, C.; Liu, L. Synergistic effect of multiple-phase rGO/CuO/Cu2O heterostructures for boosting photocatalytic activity and durability. *Appl. Surf. Sci.* **2021**, *544*, No. 148607.
(36) Liu, X.; Li, Z.; Zhao, W.; Zhao, C.; Wang, Y.; Lin, Z. A facile route to the synthesis of reduced graphene oxide-wrapped octahedral Cu_2O with enhanced photocatalytic and photovoltaic performance. *J. Mater. Chem. A* **2015**, *3*, 19148−19154.
(37) Wang, A.; Li, X.; Zhao, Y.; Wu, W.; Chen, J.; Meng, H. Preparation and characterizations of Cu_2O/reduced graphene oxide nanocomposites with high photo-catalytic performances. *Powder Technol.* **2014**, *261*, 42−48.
(38) Tran, P. D.; Batabyal, S. K.; Pramana, S. S.; Barber, J.; Wong, L. H.; Loo, S. C. A cuprous oxide-reduced graphene oxide (Cu_2O-rGO) composite photocatalyst for hydrogen generation: employing rGO as an electron acceptor to enhance the photocatalytic activity and stability of Cu_2O. *Nanoscale* **2012**, *4*, No. 3875.
(39) Wang, M.; Huang, J.; Tong, Z.; Li, W.; Chen, J. Reduced graphene oxide−cuprous oxide composite via facial deposition for photocatalytic dye-degradation. *J. Alloys Compd.* **2013**, *568*, 26−35.
(40) Abulizi, A.; Yang, G.-H.; Zhu, J.-J. One-step simple sonochemical fabrication and photocatalytic properties of Cu_2O-rGO composites. *Ultrason. Sonochem.* **2014**, *21*, 129−135.
(41) Marcano, D. C.; Kosynkin, D. V.; Berlin, J. M.; Sinitskii, A.; Sun, Z.; Slesarev, A.; Alemany, L. B.; Lu, W.; Tour, J. M. Improved Synthesis of Graphene Oxide. *ACS Nano* **2010**, *4*, 4806−4814.
(42) Jayathilaka, K. M. D. C.; Kapaklis, V.; Siripala, W.; Jayanetti, J. K. D. S. Sulfidation of electrodeposited microcrystalline/nanocrystalline cuprous oxide thin films for solar energy applications. *Semicond. Sci. Technol.* **2012**, *27*, No. 125019.
(43) Johra, F. T.; Jung, W.-G. Hydrothermally reduced graphene oxide as a supercapacitor. *Appl. Surf. Sci.* **2015**, *357*, 1911−1914.
(44) Perera, D.; Abeywickrama, A.; Zen, F.; Colavita, P. E.; Jayasundara, D. R. Evolution of oxygen functionalities in graphene oxide and its impact on structure and exfoliation: An oxidation time based study. *Mater. Chem. Phys.* **2018**, *220*, 417−425.
(45) De Silva, K. K. H.; Huang, H. H.; Yoshimura, M. Progress of reduction of graphene oxide by ascorbic acid. *Appl. Surf. Sci.* **2018**, *447*, 338−346.
(46) Upadhyay, R. K.; Soin, N.; Roy, S. S. Role of graphene/metal oxide composites as photocatalysts, adsorbents and disinfectants in water treatment: a review. *RSC Adv.* **2014**, *4*, 3823−3851.
(47) Andal, V.; Buvaneswari, G. Effect of reducing agents in the conversion of Cu 2 O nanocolloid to Cu nanocolloid. *Eng., Sci. Technol. Int. J.* **2017**, *20*, 340−344.
(48) LaGrow, A. P.; Ward, M. R.; Lloyd, D. C.; Gai, P. L.; Boyes, E. D. Visualizing the Cu/Cu2(O) Interface Transition in Nanoparticles with Environmental Scanning Transmission Electron Microscopy. *J. Am. Chem. Soc.* **2017**, *139*, 179−185.
(49) Liu, P.; Wang, H.; Li, X.; Rui, M.; Zeng, H. Localized surface plasmon resonance of Cu nanoparticles by laser ablation in liquid media. *RSC Adv.* **2015**, *5*, 79738−79745.
(50) Liu, L.; Zhang, X.; Yang, L.; Ren, L.; Wang, D.; Ye, J. Metal nanoparticles induced photocatalysis. *Nat. Sci. Rev.* **2017**, *4*, 761−780.
(51) Sönnichsen, C.; Franzl, T.; Wilk, T.; von Plessen, G.; Feldmann, J.; Wilson, O.; Mulvaney, P. Drastic reduction of plasmon damping in gold nanorods. *Phys. Rev. Lett.* **2002**, *88*, No. 077402.
(52) Wang, S.; Yi, M.; Shen, Z. The effect of surfactants and their concentration on the liquid exfoliation of graphene. *RSC Adv.* **2016**, *6*, 56705−56710.
(53) Sá, S.; Silva, H.; Brandão, L.; Sousa, J. M.; Mendes, A. Catalysts for methanol steam reforming—A review. *Appl. Catal., B* **2010**, *99*, 43−57.
(54) Zhang, X.; Peng, T.; Song, S. Recent advances in dye-sensitized semiconductor systems for photocatalytic hydrogen production. *J. Mater. Chem. A* **2016**, *4*, 2365−2402.

https://dx.doi.org/10.1021/acsanm.0c03320
ACS Appl. Nano Mater. XXXX, XXX, XXX−XXX